Transparent perovskite light-emitting diodes by employing organic-inorganic multilayer transparent top electrodes

Junqing Liang, Xiaoyang Guo, Li Song, Jie Lin, Yongsheng Hu, Nan Zhang, and Xingyuan Liu

Citation: Appl. Phys. Lett. **111**, 213301 (2017); doi: 10.1063/1.4992039
View online: https://doi.org/10.1063/1.4992039
View Table of Contents: http://aip.scitation.org/toc/apl/111/21
Published by the American Institute of Physics

Transparent perovskite light-emitting diodes by employing organic-inorganic multilayer transparent top electrodes

Junqing Liang,[1,2] Xiaoyang Guo,[1,a)] Li Song,[1,2] Jie Lin,[1] Yongsheng Hu,[1] Nan Zhang,[1] and Xingyuan Liu[1,a)]
[1]*State Key Laboratory of Luminescence and Applications, Changchun Institute of Optics, Fine Mechanics and Physics, Chinese Academy of Sciences, Changchun 130033, China*
[2]*University of Chinese Academy of Sciences, Beijing 100049, China*

(Received 26 June 2017; accepted 6 November 2017; published online 21 November 2017)

Perovskite light-emitting diodes (PeLEDs) have attracted much attention in the past two years due to their high photoluminescence quantum efficiencies and wavelength tuneable characteristics. In this work, transparent PeLEDs (TPeLEDs) have been reported with organic-inorganic multilayer transparent top electrodes that have more convenient control of the organic/electrode interface. By optimizing the thickness of the MoO_3 layer in the top electrode, the best average transmittance of 47.21% has been obtained in the TPeLED in the wavelength range of 380–780 nm. In addition, the TPeLED exhibits a maximum luminance of 6380 cd/m^2, a maximum current efficiency (CE) of 3.50 cd/A, and a maximum external quantum efficiency (EQE) of 0.85% from the bottom side together with a maximum luminance of 3380 cd/m^2, a maximum CE of 1.47 cd/A, and a maximum EQE of 0.36% from the top side. The total EQE of the TPeLED is about 86% of that of the reference device, indicating efficient TPeLED achieved in this work, which could have significant contribution to PeLEDs for see-through displays. *Published by AIP Publishing*. https://doi.org/10.1063/1.4992039

Organometal halide perovskite materials have attracted a great deal of attention over the past few years owing to their specific optoelectronic properties,[1,2] such as tuneable bandgap,[3] high carrier diffusion length,[4,5] and low exciton binding energy,[6,7] making them widely used for photovoltaic applications. Recently, organometal halide perovskite based films with high photoluminescence (PL) quantum efficiencies and narrow full width at half maximum (FWHM) have been employed for electroluminescence (EL) applications.[8–14] Encouraging performance of green emitted organic-inorganic hybrid perovskite light-emitting diodes (PeLEDs) based on $CH_3NH_3PbBr_3$ ($MAPbBr_3$) materials have been reported. A high current efficiency (CE) of 42.9 cd/A has been achieved by Cho *et al.*,[15] which boosts the research and development of PeLEDs.

For the high PL quantum efficiencies and high color purity,[16] a thin perovskite emission layer could achieve a high device performance, rendering that the device can be designed as a transparent PeLED (TPeLED) for application in see-through displays, such as window displays, automotive wind shield displays, eyeglass displays, and head-mounted displays. In a transparent light-emitting diode, light must be emitted from both sides of the device, so a transparent top electrode is of importance in the device construction, which directly determines the device performance. During the past few years, different kinds of transparent electrodes have been introduced as the transparent top electrodes into the transparent organic light-emitting diodes (OLEDs) and quantum-dot light-emitting diodes (QD-LEDs), for example, transparent conductive oxides,[17,18] graphene,[19] silver nanowires,[20] thin metal films,[21–23] and dielectric-metal-dielectric (DMD) multilayer transparent electrodes.[24–27] But actually, so far there have been few works on TPeLEDs. Therefore, the investigation of TPeLEDs will open a door for special applications of perovskite materials. For the transparent top electrodes of TPeLEDs, high transparence and low sheet resistance are two essential requirements. Moreover, the top electrodes deposited on perovskite films must be processed at low temperature since perovskite materials are sensitive to temperature.[28] Among the transparent top electrodes discussed above, DMD multilayer transparent electrodes can be highly designed to achieve high transmittance and low sheet resistance through adjusting the materials and thicknesses of the dielectric and metal layers.[29,30] For example, semi-transparent organic solar cells and semi-transparent OLED have been made by using a DMD multilayer transparent electrode.[24,31] Importantly, the DMD multilayer transparent electrodes can be thermally deposited at room temperature, which is fully compatible with perovskite processing. However, most reported DMD multilayer transparent electrodes are constructed with inorganic semiconductors as the dielectric layers, which possess high refractive indexes to ensure high transmittance; at the same time, there are also some interfacial issues introduced at the electrode/organic interface in organic material-based photoelectric devices. On the other hand, organic semiconductors have seldom been used as the dielectric layers owing to their low refractive indices, which have little help to improve the electrode transmittance. Considering that organic semiconductors have excellent mechanical flexibility and controllable energy level, which are usually employed as interfacial or carrier transport materials, then a DMD electrode with an organic dielectric layer inside and an inorganic dielectric layer outside is proposed and expected to satisfy the high transmittance requirement and at the same time form a favorable

a)Authors to whom correspondence should be addressed: guoxy@ciomp.ac.cn and liuxy@ciomp.ac.cn

electrode/organic interface in hybrid TPeLEDs that have more convenient control of interface potential barrier and better charge injection in comparison to the normal inorganic-dielectric DMD structure.

Thus, in this work, organic-inorganic multilayer transparent electrodes with the DMD structure of TPBi/LiF/Al/Ag/MoO_3were designed and employed as transparent top electrodes for TPeLEDs. The top electrodes were equipped with several properties, such as high transmittance, low sheet resistance, low temperature processing, and efficient electron injection. The optimized TPeLED shows a maximum average transmittance of 47.21% over the visible range and a maximum transmittance of 59.58% at the wavelength of 543 nm. The optimized TPeLED also exhibits good luminescent properties, with the maximum bottom and top luminance of 6380 and 3380 cd/m^2 and the maximum bottom and top CE of 3.50 and 1.47 cd/A, respectively. The proposed TPeLED in this work will provide a special application of PeLEDs, and we hope that this work can provide some exploratory effort in TPeLEDs.

Figure 1 shows the device configuration of a complete TPeLED used in this study, and the corresponding layers have been marked in the cross sectional scanning electron microscopy (SEM) image. All devices are constructed on a transparent indium tin oxide (ITO) electrode, which was cleaned with acetone, alcohol, and deionized water successively in an ultrasonic bath at 60 °C and then oven dried. Before a 40 nm-thick poly(3,4-ethylenedioxythiophene) doped with polystyrene sulfonic acid (PEDOT:PSS, Clevios P AI 4083) was spincoated on the ITO, the ITO substrate should be treated with UV-ozone for 20 min. Subsequently, the samples were baked at 140 °C for 10 min and then transferred into a nitrogen-filled glovebox. A mixture of $PbBr_2$ (Xi'an Polymer Light Technology Corp., >99.99%) and CH_3NH_3Br (Xi'an Polymer Light Technology Corp., >99.5%) in a 1:2 molar ratio dissolved in anhydrous N, N-dimethylformamide (DMF) (10 wt. %) was spincoated onto the samples (4000 rpm, 30 s). During this spincoating processing, 300 μl chlorobenzene (CB) was dropped onto the sample at about 7 s to accelerate the crystal formation. Subsequently, the samples were annealed at 80 °C for 20 min on a hot plate. The formed perovskite layer is about 60 nm-thick. Finally, TPBi (30 nm), LiF (1 nm), Al (2 nm), Ag (10 nm), and MoO_3 with different thicknesses were thermally deposited by using a vacuum deposition system at a pressure of about 3.0×10^{-4}Pa. The active area of the TPeLED was 0.12 cm^2. Before the measurement, all devices were encapsulated in the glovebox. The aforementioned device processes were carried out without exposing to air.

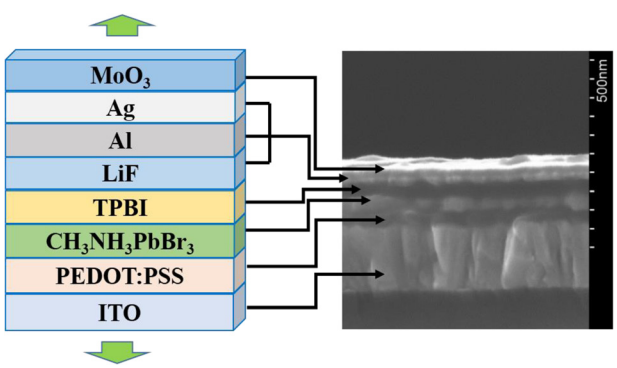

FIG. 1. Device configuration and the corresponding cross sectional SEM image of the TPeLED used in this study.

SEM images were obtained from Hitachi S4800, and X-ray diffraction (XRD) spectra were measured using a Bruker Advance D8 X-ray diffractometer. The absorption and transmission spectra were collected using a Shimadzu UV-3101PC spectrophotometer and PL spectra were measured by using a Shimadzu F-7000 spectrometer with an excitation wavelength of 360 nm. Atomic force microscopy (AFM) was carried out on a Shimadzu SPA-9700. The film thickness of each layer was measured using an Ambios XP-1 surface profiler. Current density versus voltage (J–V) and luminance versus voltage (L–V) characteristics were determined using a system combining a Keithley 2611 source-measure unit and a Konica-Minolta LS-110 Luminance Meter.

For an efficient PeLED, crystal properties and morphology control of the perovskite film are two critical issues during the PeLED processing.[9,12,13] In this work, the perovskite morphology must be controlled accurately, which would seriously affect the photoelectrical properties of the top deposited electrode. This is because a rough perovskite layer would result in a disconnected Ag layer in the top electrode followed by a failed device, whereas a smooth perovskite film favors the formation of other films on top and reduces current leakage.[32] Therefore, the optimized growth conditions of perovskite films, including the spin-coating and annealing processing, were adopted which were reported in our previous work.[33] The optimized $MAPbBr_3$ film exhibits a PL peak around 530 nm (Fig. S1 in the supplementary material), which is consistent with the other reported value.[34] The optimized $MAPbBr_3$ film also shows well crystal nature, which is revealed by the XRD measurement and shown in Fig. 2(a). In the XRD patterns, there are two sharp diffraction peaks at about 15.20° and 30.32°, which correspond to (100) and (200) planes, respectively.[15,35] The sharp diffraction peaks and the absence of the $PbBr_2$ XRD pattern suggest that the formed perovskite film has high crystal quality without any degradation.[36] Figure 2(b) shows the AFM image of the $MAPbBr_3$film used in this work. The optimized $MAPbBr_3$film is uniform and dense, with a calculated coverage of 98.2%, and the grain size distribution of $MAPbBr_3$ is concentrated around 30 nm (Fig. S2 in the supplementary material).

In TPeLEDs, transmittance and luminous efficiency are two important parameters to evaluate the EL properties. In the TPeLED construction, the ITO transparent anode and PEDOT:PSS anode interface layer remained unchanged,

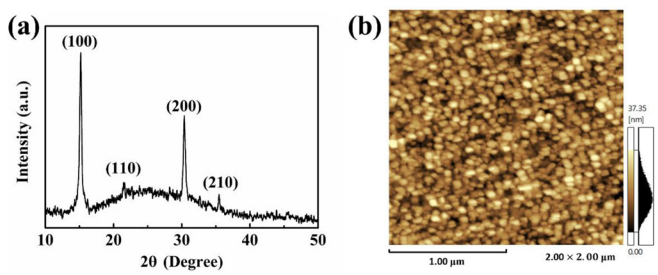

FIG. 2. (a) XRD pattern and (b) AFM image of the $MAPbBr_3$ film used in this work.

while the top transparent DMD electrode structure (TPBi/LiF/Al/Ag/MoO_3) was varied to adjust the transmittance of the whole TPeLED. As is known, the transmittance of the DMD electrode can be optimized by changing the thickness of each layer in the DMD structure, and the sheet resistance of the DMD electrode mainly depends on the thickness of metal layer.[29,30] Herein, the thicknesses of TPBi and LiF layers were the same values as the reference device, which have been optimized to ensure efficient electron injection. The metal layers were constituted by Al and Ag. An ultrathin Al (2 nm) seed layer was used to improve the transmittance by optimizing the morphology of the Ag surface.[21,22] According to our previous work, the transmittance of the DMD transparent electrode can be adjusted by changing the thicknesses of the dielectric and metal layers,[29,30] and a thinner Ag layer (less than 10 nm) would result in a large sheet resistance, while a thicker Ag layer (more than 10–12 nm) would result in a bad transmittance, so in order to obtain a high quality TPeLED, the thickness of the Ag layer was fixed at 10 nm-thick to ensure suitable sheet resistance and transmittance. It is known that MoO_3 has a high refractive index, which has been employed as the dielectric layer in DMD electrodes.[37,38] Thus, the optical transmittance of the top transparent electrode in this work was optimized by changing the thickness of MoO_3. The transmittance of the multilayer electrode that changes with varying MoO_3 thicknesses can be explicated by an optical out coupling effect based on thin-film optic theory. The optical phase thickness (δ) of thin film can be expressed as follows:[39]

$$\delta = \frac{2\pi}{\lambda} \mathrm{nd} \cos\theta, \tag{1}$$

where λ represents the wavelength of incident light, n and d denote the refractive index and thickness of the thin film, and θ is the angle of incident light. The optical thickness (nd) and optical phase thickness (δ) change with varying physical thicknesses (d) of the film. When the optical thickness is a multiple of $\lambda/2$, the transmittance of the multilayer electrode achieves the maximum value.

In order to obtain a high transmittance, a series of top electrodes with different MoO_3 thicknesses (0–122 nm) have been fabricated. Figure 3(a) shows the transmittance spectra of the top electrodes with varying MoO_3 thicknesses. It is seen that the maximum transmittance of the top electrode can be adjusted from the short wavelength region to the long wavelength region with the increase in the MoO_3 layer thickness. Figure S3 (supplementary material) shows the transmittance and reflectance changes of the top electrodes with a wide range of MoO_3 thicknesses. The transmittance value increases quickly as the MoO_3 thickness increases from 0 to 30 nm and then shows a fluctuation in a certain range and a gradual decrement trend with a further increase in the MoO_3 thickness. Compared with the transmittance values, the reflectance changes appear an opposite trend, which decreases significantly as the MoO_3 thickness increases from 0 to 30 nm and then fluctuates with the further increasing MoO_3 thickness. In order to achieve an optimized top electrode, the MoO_3 thickness was further adjusted in a narrow range of 24–40 nm, as shown in Figs. 3(b) and S4 (supplementary material). As the MoO_3 thickness increases from 24 nm to 40 nm, the transmittance of the top electrodes and the TPeLED devices presents a similar variation trend, which increases first and then decreases. A maximum average transmittance (380 nm–780 nm) of 73.48% of the top electrode was achieved with a 32 nm-thick MoO_3, and the corresponding average transmittance of the TPeLED device was 47.21%. In order to maximize the light emitting from the TPeLED, the transmittance values at the peak emission wavelength of 530 nm with different MoO_3 thicknesses are also shown in Fig. 3(b), which have a similar variation trend to the average transmittance values. The maximum transmittance values at 530 nm are 81.52% and 55.63% for the top electrode and the TPeLED device, respectively, which were also achieved with the 32 nm-thick MoO_3. The obvious decrease in the transmittance spectra of the TPeLEDs with 36 nm and 40 nm-thick MoO_3 can be attributed mainly to the absorption of the perovskite film (Fig. S5 in the supplementary material).

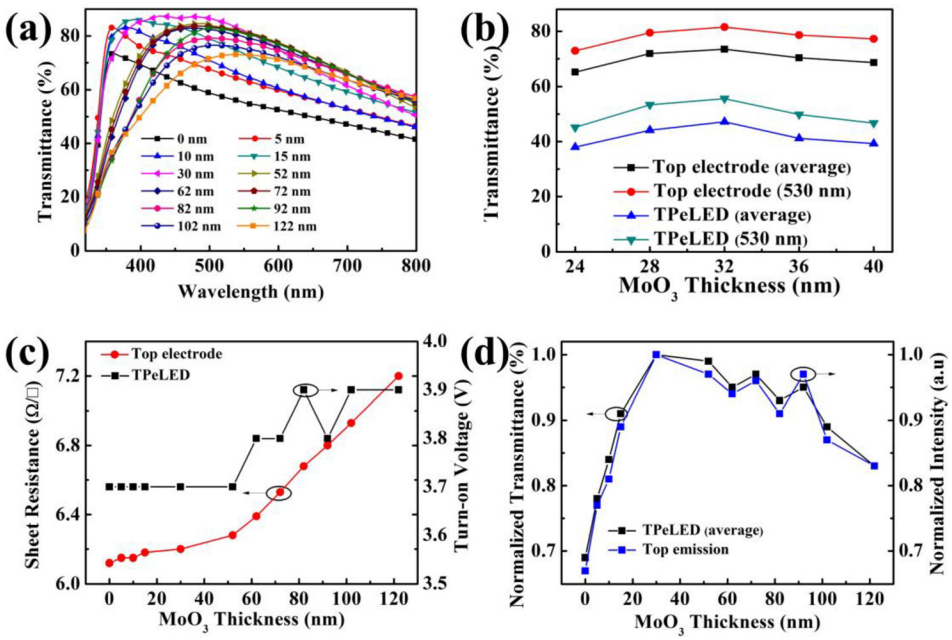

FIG. 3. (a) Transmittance spectra of the top electrodes with different MoO_3 thicknesses. (b) Transmittance variations of the top electrodes and TPeLEDs in the visible region (380 nm–780 nm) and at 530 nm with different MoO_3 thicknesses. (c) Sheet resistance variation of the top electrode and turn-on voltage variation of the TPeLEDs with different MoO_3 thicknesses. (d) Normalized average transmittance of TPeLEDs (380 nm–780 nm) and the EL emission intensity from the top electrode with different MoO_3 thicknesses.

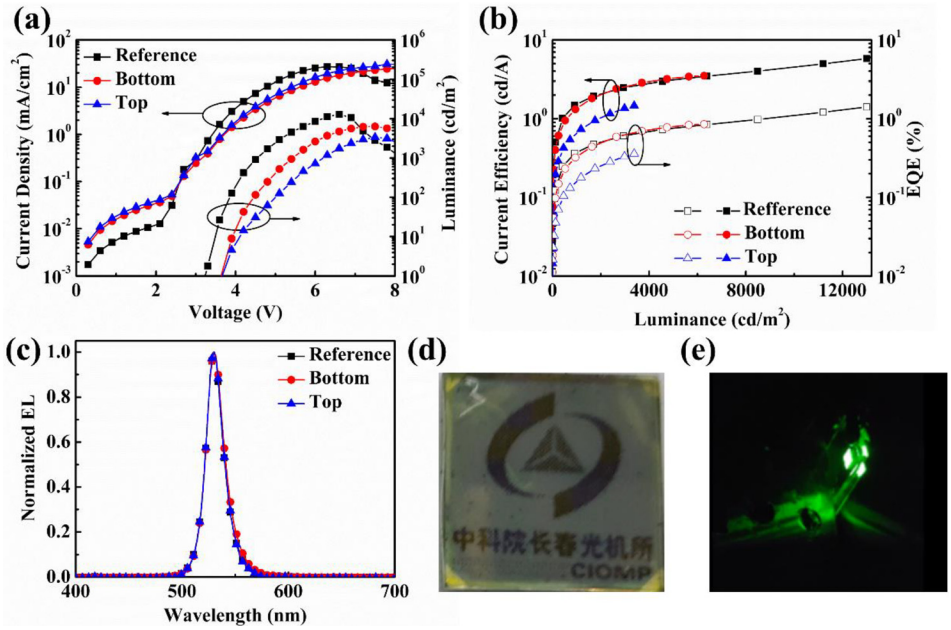

FIG. 4. (a) J-V-L characteristics of the TPeLED and reference PeLED. (b) EL efficiencies of the TPeLED and reference PeLED as a function of luminance. (c) EL spectra of the TPeLED and reference PeLED. Photographs of the TPeLED (d) before and (e) under lighting.

To further verify the effect of the MoO_3 thickness on the device performance, TPeLEDs with different MoO_3 thicknesses have been prepared, and the electrical properties of the transparent top electrode together with the device performance as a function of the MoO_3 thickness are shown in Figs. 3(c) and 3(d). Actually, the sheet resistance of the top electrode only increases slightly from 6.12 Ω/□ without MoO_3 to 7.2 Ω/□ with 122 nm-thick MoO_3. The slightly increased sheet resistance of the top electrode has no apparent effects on the carrier injection of TPeLEDs, while only the turn-on voltage of TPeLEDs increases slightly from 3.7 to 3.9 V. As seen in Fig. 3(d), the average transmittance of the TPeLEDs with different MoO_3 thicknesses shows the similar change trend to the transmittance of the top electrodes (Fig. S3 in the supplementary material), resulting in the corresponding change of EL emission intensity. Consequently, the thickness of 32 nm is the optimal one of MoO_3 for the TPeLEDs.

Figure 4(a) shows the J-V-L characteristics of the optimized TPeLED compared with the reference device, and Fig. 4(b) gives the external quantum efficiency (EQE) and CE characteristics of the TPeLED and reference PeLED as a function of luminance, respectively. The device parameters, including turn-on voltage, maximum luminance, maximum CE, and maximum EQE, are listed in Table I. From the angle-dependent emission profile of the TPeLED and reference PeLED shown in Fig. S6 (supplementary material), it is found that their emission profiles are very similar to that of Lambertian. So the EQE values listed in Table I were calculated based on this emission profile. In Fig. 4(a), the luminance measured from the bottom electrode is higher than that measured from the top electrode, resulting in higher CE and EQE from the bottom electrode [Fig. 4(b)]. In Table I, it is seen that the maximum bottom and top luminance are 6380 and 3380 cd/m^2 at 7.5 V, respectively, and the ratio of the bottom to top luminance is about 2:1. The maximum CE and EQE at the bottom side are 3.50 cd/A and 0.85%, respectively, while the maximum CE and EQE at the top side are 1.47 cd/A and 0.36%, respectively. The asymmetric light emission can be attributed to the different optical reflection of the two transparent electrodes in the TPeLED.[18,24–27] This device performance shown above is at an average level, and the EL performance of the other five devices with the same structure is listed in Table S1 (supplementary material). For comparison, a reference device with the structure of ITO/PEDOT:PSS/$MAPbBr_3$/TPBi/LiF/Al was fabricated, which is a typical bottom-emitting structure owing to the top non-transparent electrode of Al (100 nm). The reference device exhibits a maximum CE of 5.80 cd/A, a maximum luminance of 13000 cd/m^2 at 6.6 V, and a maximum EQE of 1.41%. Figure 4(c) shows EL spectra of the TPeLED and reference device. The double-side EL spectra of the TPeLED are similar to those of the reference device with an EL peak of 530 nm in accordance with the PL spectrum of the perovskite film. Although the EL performance of the TPeLED is a little poor in comparison with the reference device, the TPeLED can provide an average transmittance of 47.21% over the visible range as seen in the photographs shown in Figs. 4(d) and 4(e). Moreover, the total EQE (bottom plus top) of the TPeLED is 1.21%, which is about 86% of that of the reference device, indicating only a small amount of photon loss in the TPeLED device in comparison to the reference device. The photon loss originates likely from the difference in charge injection between the thin top contact electrode in the TPeLED and the thick one in the reference device and the difference in absorption loss between these two electrodes.

TABLE I. Device parameters of the TPeLED and the reference PeLED.

Device	Turn-on voltage (V)	Max. luminance (cd/m^2)	Max. CE (cd/A)	Max. EQE (%)
Reference	3.2	13 000	5.80	1.41
Bottom	3.7	6380	3.50	0.85
Top	3.7	3380	1.47	0.36

In summary, TPeLEDs with an organic-inorganic DMD electrode as the transparent top electrode have been proposed in this work. The transmittance of the TPeLED device can

be adjusted by changing the structure of the DMD top electrode, especially the thickness of MoO_3, and an optimized average transmittance of 47.21% over the visible range has been achieved with the maximum bottom and top luminance of 6380 and 3380 cd/m^2 at 7.5 V, respectively, together with the maximum bottom and top CE of 3.50 and 1.47 cd/A, respectively. Compared with the reference device, the total EQE of the TPeLED is 1.21%, which is about 86% of that of the reference device, illustrating small photon loss and efficient device performance in the TPeLED. We believe that the TPeLED presented in this work will be of great value for PeLED applications in see-through displays.

See supplementary material for absorption and PL spectra of the $MAPbBr_3$ film, the grain size distribution of $MAPbBr_3$ crystals in the perovskite film, optical transmittance spectra of the top electrodes with different MoO_3 thicknesses, optical transmittance spectra of ITO/PEDOT:PSS, ITO/PEDOT:PSS/$MAPbBr_3$, and TPeLED with different MoO_3 thicknesses, and angle-dependent emission profile of the devices.

This work was supported by the CAS Innovation Program, the National Natural Science Foundation of China Nos. 51503196 and 61405195, the Jilin Province Science and Technology Research Project Nos. 20170101039JC, 20150101039JC, 20160520176JH, and 20160520092JH, and project supported by the State Key Laboratory of Luminescence and Applications.

[1]G. E. Eperon, S. D. Stranks, C. Menelaou, M. B. Johnston, L. M. Herz, and H. J. Snaith, Energy Environ. Sci. **7**(3), 982 (2014).
[2]H. J. Snaith, J. Phys. Chem. Lett. **4**(21), 3623 (2013).
[3]G. Xing, N. Mathews, S. Sun, S. S. Lim, Y. M. Lam, M. Grätzel, S. Mhaisalkar, and T. C. Sum, Science **342**(6156), 344 (2013).
[4]G. Xing, N. Mathews, S. S. Lim, N. Yantara, X. Liu, D. Sabba, M. Grätzel, S. Mhaisalkar, and T. C. Sum, Nat. Mater. **13**(5), 476 (2014).
[5]S. D. Stranks, G. E. Eperon, G. Grancini, C. Menelaou, M. J. P. Alcocer, T. Leijtens, L. M. Herz, A. Petrozza, and H. J. Snaith, Science **342**(6156), 341 (2013).
[6]A. Miyata, A. Mitioglu, P. Plochocka, O. Portugall, J. T.-W. Wang, S. D. Stranks, H. J. Snaith, and R. J. Nicholas, Nat. Phys. **11**(7), 582 (2015).
[7]Q. Lin, A. Armin, R. C. R. Nagiri, P. L. Burn, and P. Meredith, Nat. Photonics **9**(2), 106 (2015).
[8]F. Deschler, M. Price, S. Pathak, L. E. Klintberg, D.-D. Jarausch, R. Higler, S. Hüttner, T. Leijtens, S. D. Stranks, and H. J. Snaith, J. Phys. Chem. Lett. **5**(8), 1421 (2014).
[9]J. C. Yu, D. B. Kim, E. D. Jung, B. R. Lee, and M. H. Song, Nanoscale **8**(13), 7036 (2016).
[10]Z.-K. Tan, R. S. Moghaddam, M. L. Lai, P. Docampo, R. Higler, F. Deschler, M. Price, A. Sadhanala, L. M. Pazos, and D. Credgington, Nat. Nanotechnol. **9**(9), 687 (2014).
[11]Y.-H. Kim, H. Cho, J. H. Heo, T.-S. Kim, N. Myoung, C.-L. Lee, S. H. Im, and T.-W. Lee, Adv. Mater. **27**(7), 1248 (2015).
[12]J. C. Yu, D. B. Kim, G. Baek, B. R. Lee, E. D. Jung, S. Lee, J. H. Chu, D.-K. Lee, K. J. Choi, and S. Cho, Adv. Mater. **27**(23), 3492 (2015).
[13]G. Li, Z.-K. Tan, D. Di, M. L. Lai, L. Jiang, J. H.-W. Lim, R. H. Friend, and N. C. Greenham, Nano Lett. **15**(4), 2640 (2015).
[14]M. Yuan, L. N. Quan, R. Comin, G. Walters, R. Sabatini, O. Voznyy, S. Hoogland, Y. Zhao, E. M. Beauregard, and P. Kanjanaboos, Nat. Nanotechnol. **11**(10), 872 (2016).
[15]H. Cho, S.-H. Jeong, M.-H. Park, Y.-H. Kim, C. Wolf, C.-L. Lee, J. H. Heo, A. Sadhanala, N. Myoung, and S. Yoo, Science **350**(6265), 1222 (2015).
[16]Z. Xiao, R. A. Kerner, L. Zhao, N. L. Tran, K. M. Lee, T.-W. Koh, G. D. Scholes, and B. P. Rand, Nat. Photonics **11**(2), 108 (2017).
[17]W. Wang, H. Peng, and S. Chen, J. Mater. Chem. C **4**(9), 1838 (2016).
[18]J.-B. Kim, J.-H. Lee, C.-K. Moon, S.-Y. Kim, and J.-J. Kim, Adv. Mater. **25**(26), 3571 (2013).
[19]J.-T. Seo, J. Han, T. Lim, K.-H. Lee, J. Hwang, H. Yang, and S. Ju, ACS Nano **8**(12), 12476 (2014).
[20]P. Jing, W. Ji, Q. Zeng, D. Li, S. Qu, J. Wang, and D. Zhang, Sci. Rep. **5**, 12499 (2015).
[21]J. W. Huh, J. Moon, J. W. Lee, J. Lee, D.-H. Cho, J.-W. Shin, J.-H. Han, J. Hwang, C. W. Joo, and J.-I. Lee, Org. Electron. **14**(8), 2039 (2013).
[22]J. H. Im, K.-T. Kang, S. H. Lee, J. Y. Hwang, H. Kang, and K. H. Cho, Org. Electron. **33**, 116 (2016).
[23]H.-M. Kim, A. R. B. Mohd Yusoff, T.-W. Kim, Y.-G. Seol, H.-P. Kim, and J. Jang, J. Mater. Chem. C **2**(12), 2259 (2014).
[24]K. Hong, K. Kim, S. Kim, I. Lee, H. Cho, S. Yoo, H. W. Choi, N.-Y. Lee, Y.-H. Tak, and J.-L. Lee, J. Phys. Chem. C **115**(8), 3453 (2011).
[25]B. Tian, G. Williams, D. Ban, and H. Aziz, J. Appl. Phys. **110**(10), 104507 (2011).
[26]S. D. Yambem, M. Ullah, K. Tandy, P. L. Burn, and E. B. Namdas, Laser Photonics Rev. **8**(1), 165 (2014).
[27]F. Fries, M. Fröbel, S. Lenk, and S. Reineke, Org. Electron. **41**, 315 (2017).
[28]H.-L. Hsu, C.-P. Chen, J.-Y. Chang, Y.-Y. Yu, and Y.-K. Shen, Nanoscale **6**(17), 10281 (2014).
[29]X. Guo, J. Lin, H. Chen, X. Zhang, Y. Fan, J. Luo, and X. Liu, J. Mater. Chem. **22**(33), 17176 (2012).
[30]Z. Xue, X. Liu, N. Zhang, H. Chen, X. Zheng, H. Wang, and X. Guo, ACS Appl. Mater. Interfaces **6**(18), 16403 (2014).
[31]H. Lin, L. Zhu, H. Huang, C. J. Reckmeier, C. Liang, A. L. Rogach, and W. C. H. Choy, Nanoscale **8**(47), 19846 (2016).
[32]X. Ren, X. Li, and W. C. H. Choy, Nano Energy **17**, 187 (2015).
[33]J. Liang, Y. Zhang, X. Guo, Z. Gan, J. Lin, Y. Fan, and X. Liu, RSC Adv. **6**(75), 71070 (2016).
[34]Z. Wang, T. Cheng, F. Wang, S. Dai, and Z. Tan, Small **12**(32), 4412 (2016).
[35]N. Wang, L. Cheng, J. Si, X. Liang, Y. Jin, J. Wang, and W. Huang, Appl. Phys. Lett. **108**(14), 141102 (2016).
[36]X. Fang, K. Zhang, Y. Li, L. Yao, Y. Zhang, Y. Wang, W. Zhai, L. Tao, H. Du, and G. Ran, Appl. Phys. Lett. **108**(7), 071109 (2016).
[37]D.-T. Nguyen, S. Vedraine, L. Cattin, P. Torchio, M. Morsli, F. Flory, and J. C. Bernède, J. Appl. Phys. **112**(6), 063505 (2012).
[38]T. Abachi, L. Cattin, G. Louarn, Y. Lare, A. Bou, M. Makha, P. Torchio, M. Fleury, M. Morsli, and M. Addou, Thin Solid Films **545**, 438 (2013).
[39]H. A. Macleod, *Thin-Film Optical Filters*, 4th ed. (CRC Press, New York, USA, 2010).